Hydrol. Earth Syst. Sci. Discuss., 6, 1939–1972, 2009
www.hydrol-earth-syst-sci-discuss.net/6/1939/2009/

Hydrology and Earth System Sciences Discussions

Papers published in *Hydrology and Earth System Sciences Discussions* are under open-access review for the journal *Hydrology and Earth System Sciences*

Seasonal and diurnal variations in moisture, heat and CO_2 fluxes over a typical steppe prairie in Inner Mongolia, China

Z. Gao[1,2], D. H. Lenschow[3], Z. He[4], M. Zhou[1,5], L. Wang[1], Y. Wang[6], J. He[6], and J. Shi[6]

[1]State Key Laboratory of Atmospheric Boundary Layer Physics and Atmospheric Chemistry, Institute of Atmospheric Physics, CAS, Beijing, China
[2]State Key Laboratory of Severe Weather, Chinese Academy of Meteorological Science, CMA, Beijing, China
[3]National Center for Atmospheric Research (NCAR), Boulder CO, USA
[4]Institute of Atmospheric Sciences, Nanjing University of Information Science and Technology, Nanjing, China

[5] Key Laboratory for Polar Science, Polar Research Institute of China, Shanghai, China
[6] Xilinhaote Meteorological Station, Inner Mongolia, China

Received: 28 January 2009 – Accepted: 3 February 2009 – Published: 6 March 2009

Correspondence to: Z. Gao (zgao@mail.iap.ac.cn)

Published by Copernicus Publications on behalf of the European Geosciences Union.

Abstract

In order to examine energy partitioning and CO_2 exchange over a steppe prairie in Inner Mongolia, China, fluxes of moisture, heat and CO_2 in the surface layer from June 2007 through June 2008 were calculated using the eddy covariance method. The study site was homogenous and approximately 1500 m × 1500 m in size. Seasonal and diurnal variations in radiation components, energy components and CO_2 fluxes are examined. Results show that all four radiation components changed seasonally, resulting in a seasonal variation in net radiation. The radiation components also changed diurnally. Winter surface albedo was higher than summer surface albedo because during winter the snow-covered surface increased the surface albedo. The seasonal variations in both sensible heat and CO_2 fluxes were stronger than those of latent heat and soil heat fluxes. This implies that both sensible heat and CO_2 fluxes may be more significant climate signals than latent heat and soil fluxes. Sensible heat flux was the main consumer of available energy for the entire experimental period. The energy imbalance problem was encountered and the causes are analyzed.

1 Introduction

The relatively recent increase in atmospheric carbon dioxide (hereinafter, referred to as CO_2) concentration has profound implications for the planet's climate (see, for example, the IPCC report) as well as on photosynthesis and the structure and function of plant communities, Vegetation therefore plays a crucial role in the global carbon balance (Woodward et al., 1998; Mielnick et al., 2001). The energy budget balance over land surfaces is the most important of all the ecological processes related to carbon sequestration in terrestrial ecosystems (Baldocchi et al., 1997; Dugas et al., 1999; Hao et al., 2007). Surface fluxes of momentum, heat and moisture determine to a large extent the steady state of the atmosphere (Beljaars and Holtslag, 1991). Climate simulations are especially sensitive to the seasonal and diurnal variations in surface partitioning of

HESSD

6, 1939–1972, 2009

available energy into sensible and latent heat fluxes (e.g., Rowntree, 1991; Dickinson et al., 1991).

In order to evaluate the long-term energy balance and evapotranspiration, a number of experimental studies have been carried out on various terrestrial surfaces such as forest, grasslands and paddy fields throughout the world during the past decade (e.g., Baldocchi and Vogel, 1997; Toda et al., 2002; Gao et al., 2003; Bi et al., 2006; Hao et al., 2007). Previous work has reported on measurements of the seasonal and/or diurnal variations of heat, water vapor and CO_2 exchanges over different land surfaces in a variety of ecosystems ranging from the tropics to the northern high latitudes (e.g., Hartog et al., 1994; Delire et al., 1995; Betts et al., 1995; Campbell et al., 2001; Vourlitis et al., 2001; Merquiol et al., 2002; Xue et al., 2004; Barros et al., 2005; Steven et al., 2005; Bi et al., 2006; Hao et al., 2007).

Grasslands are approximately 32% of the Earth's natural vegetation (Adams et al., 1990) and grassland ecosystems undergo considerable annual fluctuations in gross primary production (Frank and Dugas, 2001); grassland ecosystems also significantly and asymmetrically respond to climate change and pertinent biomass dynamics (Baldocchi et al., 2001; Wever et al., 2002). Prior researchers mainly paid attention to savanna areas and the Central Great Plains of the US (Dugas et al., 1999; Frank and Dugas, 2001; Sims and Bradford, 2001; Suyker and Verma, 2001; Novick et al., 2004). In contrast, there are few works focused on measurements of the seasonal and/or diurnal variations of heat, water vapor and CO_2 exchanges in the great steppes of Asia (Li et al., 2006; Hao et al., 2007) because much of the data obtained so far is still insufficient.

We conducted a micrometeorological experiment over a natural steppe prairie in Inner Mongolia from June 2007 to improve the current understanding of energy partitioning and CO_2 exchange over a typical steppe prairie in Inner Mongolia and to find which surface energy components show the strongest climate signals. The main objective of the present work is therefore to quantify the seasonal and diurnal variations in energy and CO_2 exchanges over the above mentioned surface using eddy covariance

techniques.

2 Materials and methods

2.1 Site

Measurements have been collected at a grassland site (44° 08′ 31″ N, 116° 18′ 45″ E, 1160.8 m above sea level) in the typical steppe prairie in Inner Mongolia since 1 June 2007. The field has reverted to its natural status in the past 50 years. Similar to the site of Hao et al. (2007), the xeric rhizomatous grass Leymus chinensis is the constructive species, and Agropyron cristatum, Cleistogenes squarrosa, and Carex duriuscula are the dominant species at our site. The heights of grass clumps are about 0.50–0.70 m, and coverage fraction depends on annual precipitation, ranging from 30% to 70%. Soil at the site was predominantly dark chestnut (Mollisol) soil with rapid drainage of water. It has only a thin layer of humus (the organic portion of the soil created by partial decomposition of plant or animal matters) which provides vegetation with nutrients.

This site is smooth, homogeneous and approximately 1500 m × 1500 m, surrounded by low hills whose heights are lower than 30 m with slopes less than 5°. Unfortunately, the leaf area index (LAI) has not been measured. This site has a semi-arid continental temperate steppe climate with a dry spring, autumn, humid summer and snow-covered winter. The average annual temperature is about 272.5 K, with a growing season of 150–180 days. The annual precipitation range is 320–400 mm, and rainfall is concentrated within the period from June to August (Hao et al., 2007).

2.2 Micrometeorological measurements

(i) Fast response measurements.

A three-dimensional sonic anemometer (CSAT3, Campbell Scientific Inc.) was used to measure the means and standard deviations of wind velocity components (i.e., u, v

and w) and air temperature (T), and a LI-7500 (LiCor, USA) gas analyzer was used to measure the mean and standard deviations of water vapor density and CO_2. The gas analyzer was calibrated before the experiment using three values of standard gases (between 300 and 400 ppmv CO_2 in N_2). These sensors were installed on a mast at 4.0 m above the ground (Fig. 1). The sensor outputs were recorded at a sampling rate of 10 Hz and were averaged over 30 min periods. Appropriate corrections were made for non-zero mean vertical velocity. Following Moore (1986), we corrected eddy covariance values for the effects of path length averaging of the sonic anemometer and the gas analyzer, and for the spatial separation of sensors. Corrections were made for density fluctuations in calculating the fluxes of water vapor and CO_2 (Webb et al., 1980).

We eliminated outliers from 30-min measurements of turbulence by using a criterion of $X(t)<(\overline{X}-4\sigma)$ or $X(t)>(\overline{X}+4\sigma)$, where $X(t)$ denotes the measurement (i.e., wind speed components, temperature), $\overline{X}$ is the mean over the interval and σ the standard deviation. Data during and after rain events was removed because the sonic anemometer could malfunction in these cases. Any gaps were filled by linear interpolation.

(ii) Slow response measurements

Other supporting data were collected during the experiment. Soil heat flux was measured by embedding two heat flux plates (HFT-3, Campbell Scientific Inc.) at a depth of 0.01 m. Soil temperature was measured at 6 depths (surface, 0.05, 0.10, 0.15, 0.20, and 0.40 m) in the soil. Upward and downward short- and long-wave radiation components were measured with radiometers (model 2AP Tracker, Kipp & Zonen Inc.) mounted at a height of 2.0 m. The data were recorded by a Datataker (CR5000, Campbell Scientific Inc.) with a PCMCIA memory card. The data were sampled each minute and averages recorded every 10 min.

The set of observational data includes the following meteorological quantities: horizontal wind speed, air temperature, specific humidity, air pressure and precipitation. Figure 2 shows the time series of (a) weekly mean wind vector (WV in $m\,s^{-1}$), (b) weekly mean air temperature (T_{air} in K), (c) weekly mean specific humidity (q in $g\,kg^{-1}$),

(d) daily mean air pressure (P in hpa), and (e) daily precipitation (Prec. in mm day^{-1}) obtained since June 2007. It is obvious that all of these meteorological quantities undergo a marked seasonal cycle. In the wet season (June through August), high temperature, high humidity, and low wind speed were coincident with low air pressure and precipitation events were frequent. The reverse occurred during the dry season.

The plots in Fig. 2a–c are derived from the fast response measurements. The composition method is applied for estimation of daily variation for each week and then a weekly average is calculated. The gaps in Fig. 2 were caused by power outages at the site. The plots in Fig. 2d–e are derived from the slow response instruments.

Our site is located in a mid-latitude semi-arid continental temperate and westerlies climate zone. During the winter, cold dry air always came from the southwest, significantly influencing the area. Because of the influence of the temperate monsoon climate, the south to southwest wind was maintained through whole experimental period. Although the annual mean wind speed was about 3.0 m s^{-1} (shown in Fig. 2a), the maximum hourly mean wind speed reached 8 m s^{-1}

The seasonal variation of air temperature (T_{air}) was remarkable. Monthly mean air temperature reached a maximum (295.0 K) in July and August, and the lowest air temperature (252.0 K) occurred in the middle of December. The difference between the highest air temperature and lowest air temperature was 43 K for the whole experimental period and the annual mean air temperature was 277.5 K. Similar seasonal variation occurred in specific humidity (q), with the correlation coefficient between q and T_{air} reaching 0.82. Specific humidity varied also in response to variations in precipitation (Fig. 2c and e). Because of the semi-arid continental temperate climate, q is always less than 12 g kg^{-1}, and less than 5 g kg^{-1} during the period from October 2007 to April 2008.

Air pressure varied seasonally but in reverse phase to air temperature and specific humidity. Almost all precipitation occurred from June to August 2007 and in June 2008. Snow occurred during the periods: 2–10 December 2007, 21, 29 January, and 15, 24, 27–30 March 2008.

HESSD
6, 1939–1972, 2009

2.3 Theoretical considerations

The surface energy balance over the grass canopy can be approximated by:

$$Rn = H + LE + G_0 + Re, \quad (1)$$

where Rn is the net radiation, H and LE are the sensible heat and latent heat fluxes, respectively, G_0 is the soil heat flux at the surface, and Re is the residual energy involved in various processes, such as photosynthesis and respiration (Harazono et al., 1998; Burba et al., 1999). We determine Re from the formula: Re=Rn−(H+LE+G_0). Rn was measured using slow response instruments (described above). Eddy fluxes of sensible heat and latent heat were calculated as (e.g., Kaimal and Finnigan, 1994):

$$H = \overline{\rho} C_p \overline{w'T'}, \quad (2)$$

$$LE = L\overline{\rho}\,\overline{w'q'}, \quad (3)$$

where $\overline{\rho}$, C_p and L are the density of air (kg m^{-3}), the specific heat of air (J kg^{-1} K^{-1}), and the latent heat of vaporization (J kg^{-1}), respectively. w', T' and q' are the fluctuations in the vertical wind component (m s^{-1}), air temperature (K) and specific humidity, respectively.

G_0 is estimated by using a combination of soil calorimetry and measurement of the heat flux density at depth of 0.1 m using heat flow transducers. The heat storage of the soil layer above the plate is included as follows,

$$G_0 = G_1 + C_g \Delta z \delta T / \delta t, \quad (4)$$

where G_1 is the soil heat flux at depth of 0.1 m, Cg the volumetric heat capacity of the soil, which can be easily derived from soil components (Gao, 2005), Δz the thickness of a thin layer of the soil, T the mean soil temperature of the thin layer, δT the change in mean soil temperature during the measurement period, and δt the change in time.

Since the 1980s, the development of fast response CO_2 analyzers has enabled us to directly measure CO_2 fluxes over rice canopies using eddy covariance methods:

$$F_c = \overline{w'c'}, \quad (5)$$

where F_c is CO_2 flux ($mg\,m^{-2}\,s^{-1}$) and c' is the fluctuation in the concentration of CO_2 ($mg\,m^{-3}$) (Desai et al., 2008).

The ratio of the sum of sensible and latent heat fluxes ($H+LE$) to available energy (the difference of net radiation and soil heat flux: $Rn-G_0$) is presented to examine the surface heating rate ε.

Horst and Weil (1994) documented the stability dependency of footprint. The adequacy of the fetch may be confirmed by footprint analysis for neutral flow (e.g., Schuepp et al., 1990; Harazono et al., 1998). The cumulative normalized contribution to the surface flux from upwind locations, $C_F(\chi_L)$, can be expressed as

$$C_F(\chi_L) = \exp[-U(z-d)/ku_*\chi_L], \quad (6)$$

where d is the zero plane displacement, k is von Karman's constant, u_* is the friction velocity, χ_L is the distance upwind of the measuring point, and U is the average wind speed between the surface and observation height z. Assuming a logarithmic profile for horizontal wind speed $u(z)$, with z, U is given by $U = \int_{d+z_0}^{z} u(z)dz / \int_{d+z_0}^{z} dz = \frac{u_*[\ln((z-d)/z_0)-1+z_0/(z-d)]}{k(1-z_0/(z-d))}$. The code from Schmid et al. (1994) is publicly available (http://www.indiana.edu/~climate/SAM/SAM_FSAM.html) and was used in this study.

3 Results and discussion

3.1 Footprint analysis

Data were collected at 4 m above the ground surface, which is higher than three times of the maximum height (0.6 m) of the grass clumps on the Steppe. Thus the flow

assumes the properties of the conventional atmospheric surface layer such as the constant flux region. To estimate the average footprint for whose experiment, the contributions of the cumulative flux were computed using Eq. (6), where U=3.98 m s^{-1}, z=4.0 m, d=0.2 m, and u_*=0.30 m s^{-1}. Our analysis (Fig. 3) indicates that approximately 90% of the measured flux at the measurement height was expected to come from within the nearest 1100 m of upwind area for neutral stability during the entire period. The footprint flux distribution shows the maximum source weight location is 60 m upwind from the mast.

3.2 Seasonal variations on a weekly average basis

3.2.1 Radiation components

Figure 4 shows the seasonal variation of the four radiation components: (a) downward shortwave radiation (hereinafter, referred to as DSR), (b) upward shortwave radiation (USR), (c) downward longwave radiation (DLR), (d) upward longwave radiation (ULR), and (e) albedo of the underlying surface, defined as the ratio of the maximum values of USR and DSR. The seasonal variations of DSR, DLR and ULR were similar. They maintained high values during the summer and low values during the winter. The seasonal variation of USR had not been obvious when ground was not snow-covered and the seasonal variation of albedo was relatively constant at 0.22. After snow occurred, USR increased and the albedo drastically increased.

The consistent seasonal variation T_{air}, q, P, Prec., DSR, DLR, and ULR are shown in Figs. 2 and 4.

3.2.2 Energy components and CO_2 flux

Figure 5 shows the seasonal variation of weekly means of (a) net radiation (Rn), (b) sensible heat flux (H), (c) latent heat flux (LE), (d) soil surface heat flux (G_0), and (e) CO_2 flux (F_{CO_2}). Rn was calculated by using the four radiation components (i.e., DSR,

USR, DLR, and ULR). H, LE and F_{CO_2} were measured by fast response instruments and calculated using Eqs. (2), (3) and (5). Gaps occurring in H, LE, G_0 and F_{CO_2} were caused by instrument problems.

Rn, H, LE, G_0, and F_{CO_2} all showed remarkable seasonal variation. The negative sign in F_{CO_2} means that surface vegetation absorbed CO_2. The variations in Rn, H, LE, G_0 and F_{CO_2} are generally consistent; however the weekly oscillation in LE was weaker than those in Rn, H, and F_{CO_2}. The sensible heat flux was the main consumer of surface available energy (Rn–G_0). The grass grew well in the summer, and the strong photosynthesis led to the larger water vapor release and the larger negative F_{CO_2}. G_0 was about several watts per square meter on average. During December 2007 when ground was covered by snow: (1) Rn was negative; (2) the grass was short and senescent, and CO_2 absorption therefore decreased; (3) the snow surface absorbed sensible heat flux from the air; (4) LE was close to zero; and (5) G_0 was almost constant (negative several watts per square meters).

3.3 Diurnal variations on monthly average basis

3.3.1 Radiation components

In order to investigate the diurnal variation of the radiation components, the monthly means of the diurnal variation in the radiation components (DSR, USR, DLR, and ULR) are given in Fig. 6 where a composite analysis method is used and the short lines are error bars. We find that diurnal variations in DSR, USR and ULR occurred in all months, whereas diurnal variations in DLR were not significant from November 2007 to February, 2008. Diurnal variations in DSR and ULR were large in summer, but weaker in winter. On average, the maximum values of DSR and ULR occurred in June 2007 and reached 804.4 $W\,m^{-2}$ and 558.1 $W\,m^{-2}$, respectively. The minimum values of DSR and ULR occurred in December 2007, and reached 354.9 $W\,m^{-2}$ and 264.7 $W\,m^{-2}$, respectively. The maximum value of DLR occurred in July 2007, and reached 371.2 $W\,m^{-2}$. The maximum value of USR occurred in February 2008 and

HESSD
6, 1939–1972, 2009

reached 257.8 W m^{-2} and the minimum value of USR occurred in November 2007 and reached 144.4 W m^{-2}. The large USR occurring from December 2007 through February 2008 were caused by large albedo of the snow-covered surface, resulting in the large surface albedo shown in Fig. 6e. It is a clear indication that the albedo of fresh snow was higher than 0.64.

3.3.2 Energy components

The monthly mean diurnal variation courses of net radiation (*Rn*), sensible heat flux (*H*), latent heat flux (*LE*), soil heat flux (G_0), and CO_2 flux (F_{CO_2}) for all clear days are given in Fig. 7 where a composite analysis method is used and the short lines are error bars. Figure 7a shows that the diurnal variation pattern of *Rn* is similar to that of DSR, i.e., the diurnal variation was significant in summer and weak in winter. The maximum diurnal variation occurred in July and the peak value of *Rn* reached 488.8 W m^{-2}. The minimum diurnal variation occurred in January 2008 and the peak value of *Rn* was 115.3 W m^{-2}.

Figure 7b shows that seasonal variations in sensible heat flux were stronger than those in *LE*. The maximum value of *H* occurred in May 2008 and reached 302.6 W m^{-2} and the minimum value of *H* occurred in December 2007 and was 54.4 W m^{-2}.

Figure 7c shows that the seasonal variation in latent heat flux was remarkable. Obvious diurnal variation of *LE* occurred in summertime, with a maximum value of 106.8 W m^{-2} occurring in June 2008. Diurnal variation of *LE* was not significant in wintertime and the maximum value was 30.0 W m^{-2} which occurred in January 2008. Obvious diurnal variation of *LE* in summer might be attributed to the following: (1) precipitation frequently occurred (as shown in Fig. 2) and steppe grass grew well in summer, and (2) the diurnal variation in net radiation was large in summer (as shown in Fig. 7a).

Figure 7d shows the seasonal variation of soil surface heat flux (G_0). Hao et al. (2007) investigated the soil heat flux measured at 0.05 m depth and did not find

obvious diurnal variations in their selected four periods (i.e., pre-growth, growth, post-growth, and frozen soil) at their steppe site in Inner Mongolia. Our Fig. 7d shows that there is significant diurnal variation in G_0. The difference of our results from those by Hao et al. (2007) can be attributed to two facts: (1) Hao et al. (2007) neglected the soil heat storage in the soil layer ranged from surface to 0.05 m depth. Our analysis shows that the soil heat storage in the shallow surface layer diurnally changed on clear days; and (2) we selected only clear days for analysis, but Hao et al. (2007) used all data for their investigation. Soil heat flux is very low or questionable on rainy or cloudy days.

Figure 7e shows that the seasonal variation of F_{CO_2} was similar to that of H and LE, but in the reverse phase. The most significant diurnal variation occurred in May 2008 when the steppe grass was luxuriant. The peak value reached $-0.69\,mg\,m^{-2}\,s^{-1}$. Weak diurnal variation occurred in December 2007 when the grass was senescent and the peak value was only $-0.21\,mg\,m^{-2}\,s^{-1}$.

In summary, Figs. 5 and 7 show that the seasonal and diurnal variations in H and F_{CO_2} are larger than those in LE and G_0, which implies that both H and F_{CO_2} may be more significant climate indicators than LE and G_0. Hao et al. (2007) investigated diurnal variations in H, LE and G_0, and found LE was larger than H during growth (in 2003 and 2004) and post-growth seasons (in 2004). The reason is that precipitation was frequent in 2003 and 2004, which can be seen in their Fig. 2, and precipitation caused high surface evaporation in their experiment areas. Bi et al. (2007) examined energy partitioning and CO_2 exchange over grassland in the tropical monsoon environment of southern China by using H, LE, and F_{CO_2} measured in the near-surface layer from May 2004 to July 2005. They found both LE and F_{CO_2} may be more significant climate indicators than $H$and G_0 in that area.

3.4 Energy partitioning

The monthly means of the Bowen ratio ($\beta \equiv H/LE$) were 3.25, 3.25, 3.28, 3.34, 3.44, 3.49, 3.56, 3.61, 3.54, 3.41, 3.32, 3.25 and 3.21 from June 2007 to June 2008. It is obvious that the sensible heat flux was the main consumer of available energy ($Rn-G_0$)

for all the year round in this arid and semiarid area. Taking a yearly average, the Bowen ratio was 3.38, H/Rn=62%, LE/Rn=18%, G_0/Rn=9%, and Re/Rn=11%. Because the site was covered by grass, the residual energy (Re) is mainly the heat storage in the grass. The proportion of sensible heat flux in net radiation, H/Rn reached the maximum value (0.63) in June through August 2007 and May through June in 2008 and reached the minimum value of 0.61 in December 2007. H/Rn was lower than 0.62 during the period from October 2007 to February 2008, and was larger than 0.62 during summer 2007. The proportion of latent heat flux in net radiation, LE/Rn, reached a maximum value (0.19) in June 2008, and reached a minimum value (0.17) in January 2008. LE/Rn was less than 0.18 during the period from October 2007 through February 2008, and was larger than 0.18 for the rest of the time.

Figure 8 shows the intercomparison of $H+LE$ and $Rn-G_0$. The surface heating rate ε is 0.93 and the correlation coefficient between $H+LE$ and $Rn-G_0$ is 0.85. Wever et al. (2002) examined the energy balance over a northern temperate grassland near Lethbridge, Alta., Canada, and found that the slope of the relationship between $H+LE$ and $Rn-G_0$ ranged from 0.87 to 0.90. Hao et al. (2007) used soil heat flux measured at 0.05 m depth rather than soil surface heat flux for energy balance analysis, and found that $H+LE$=0.69($Rn-G$)+17.09. Their failure to close the energy budget may be partly attributed to neglecting soil and vegetation heat storage.

Our analysis of the surface heating rate is focused on the data collected on rain-free days, because the sonic anemometer malfunctions during and after rain events.

Theoretically, ε should be very close to 1.0. The energy imbalance that occurred for these measurements is unexpected because the experiment was carried out over a relatively flat, homogeneous site with sufficient fetch and the flux calculations are rigorous. Such energy imbalances have also been encountered in other major field campaigns and caused difficulty for their climate applications (e.g., Kahan et al., 2006). Previous researchers (Foken and Oncley, 1995; Panin et al., 1996; Wicke and Bernhofer, 1996; Foken et al., 1999; Kahan et al., 2006; Oncley et al., 2007; Su et al., 2008) concluded that the causes of the imbalance of the energy budget were usually related to the er-

rors/uncertainties in the individual energy component measurements and the influence of different footprints on the individual energy components. For our site, the difference in phases of *Rn*, *H*, *LE* and G_0 (Gao et al., 2009), and the unavoidable uncertainties that occurred in the individual energy component measurements are the main causes of the energy imbalance encountered.

3.5 Soil temperature

Surface radiation and energy budget balances are related to variations in soil temperature and soil water content. Figure 9 shows the seasonal variation of half-hourly-mean soil temperatures at soil surface and five depths (0.05, 0.10, 0.15, 0.20, and 0.40 m), and water content at three depths (0.10, 0.20, and 0.50 m). The seasonal variation trends of soil temperature and water content are close to that of air temperature. The soil surface temperature is derived from ULR where the infrared emissivity is assumed to be 0.98 (Garratt, 1992).

As may be expected, the seasonal variations in soil temperature and water content in shallow layers were large There is evidence of seasonal variation in soil temperature measured at 0.40 m depth. In general the range of seasonal variations measured in the deep layer was much less than those of soil temperature and water content measured in the shallower layers. The high soil temperatures occurred during summer (June–August), and low soil temperature occurred in January and February. The difference between the annual highest and lowest soil temperature ranged from 38 K to 59 K for these depths. Soil water content at 0.10 m depth sensitively responded to precipitation with the most striking case happening on 3 August 2007 when a thunderstorm made the greatest sudden change of soil wetness.

We also examined the diurnal variation of soil temperatures. Results show that soil temperatures diurnally changed in shallow layers, diurnal variation trends weakened with increasing depth and almost no diurnal variation occurred with soil temperature measured at a depth of 0.4 m.

3.6 Case study of diurnal cycles

In this section we investigate the diurnal cycle of the radiation components, energy fluxes, CO_2 flux, and energy balance for clear days under specific shortwave radiation environments: (1) on 7 June 2008, the daily downward shortwave radiation reached the largest value of our experimental period; and (2) On 22 December 2007, the albedo daily upward shortwave radiation reached the largest value of our experimental period. Figure 10 shows the diurnal cycle of radiation components for these two days, and the corresponding daytime surface albedo.

The maximum values of downward shortwave radiation and upward shortwave radiation were 1020 $W\,m^{-2}$ and 229 $W\,m^{-2}$, respectively, on 7 June 2008; 424 $W\,m^{-2}$ and 304 $W\,m^{-2}$, respectively, on 22 December 2007. The corresponding surface albedo values were 0.22 and 0.70, respectively. The winter surface albedo is higher than the summer surface albedo because of snowfall.

The downward longwave radiation components on 7 June 2008 were greater than those on 22 December 2007, and both of them showed almost no daily change. The upward shortwave radiation component on 7 June 2008 diurnally changed in contrast to that on 22 December 2007. Similar to Fig. 10, the daily cycles of the energy flux components and CO_2 flux for the two days mentioned above were plotted in Fig. 11. The maximum values of net radiation (Rn), sensible heat (H), latent heat (LE), soil heat (G_0), and CO_2 (F_{CO_2}) fluxes were 564.0 $W\,m^{-2}$, 294.5 $W\,m^{-2}$, 141.9 $W\,m^{-2}$, 168.1 $W\,m^{-2}$ and 0.63 $mg\,m^{-2}\,s^{-1}$ on 7 June 2008. The maximum values of Rn, H, LE, G_0, and F_{CO_2} were 34.0 $W\,m^{-2}$, 20.2 $W\,m^{-2}$, 9.8 $W\,m^{-2}$, 19.2 $W\,m^{-2}$ and 0.07 $mg\,m^{-2}\,s^{-1}$ on 22 December 2007. On 7 June 2008, the sensible heat flux was larger than the latent heat flux; and on 22 December 2007, the sensible heat flux and latent heat flux were close to zero. On 7 June 2008, the daytime CO_2 absorption was significant because of the strong photosynthesis associated with the grass, and on 22 December 2007, the daytime CO_2 absorption was close to zero owing to snow-covered surface.

Figure 12 shows the energy partitioning for 7 June 2008 and 22 December 2007.

HESSD
6, 1939–1972, 2009

Sensible heat fluxes were 90.3 $W m^{-2}$ and −17.4 $W m^{-2}$; latent heat fluxes were 58.2 $W m^{-2}$ and −0.71 $W m^{-2}$; soil heat fluxes were 21.9 $W m^{-2}$ and −5.8 $W m^{-2}$; and residual heat fluxes were −3.2 $W m^{-2}$ and −12.4 $W m^{-2}$ for 7 June 2008 and 22 December 2007, respectively.

4 Summary and conclusions

In order to investigate energy partitioning and CO_2 exchange over the land surface in a northern arid climate environment and to investigate which surface energy components are strong climate signals, eddy covariance measurements of moisture, heat and CO_2 fluxes over steppe prairie in Inner Mongolia, China were carried out from June 2007 through June 2008.

All four radiation components seasonally changed, resulting in a seasonal variation in net radiation. The components also changed diurnally. Winter surface albedo was higher than summer surface albedo, because in winter the surface was covered by snow.

Appropriate correction was made for turbulent fluxes. The seasonal variations in both sensible heat and CO_2 fluxes were stronger than those in latent heat and soil heat fluxes, which implies that both sensible heat and CO_2 fluxes may be more significant climate signals than latent heat and soil fluxes. Sensible heat flux was the main consumer of available energy for the entire experimental period.

Surface energy partitioning was examined and the surface heating rate (ε) was found to be 0.93 during the experiment. The energy imbalance problem was encountered. The main causes of the energy imbalance encountered were thought to be the difference in phases of Rn,H, LE and G_0 (Gao et al., 2009), and the unavoidable uncertainties that occurred in the individual energy component measurements.

Acknowledgements. This study was mainly supported by MOST (2006CB400600, 2006CB403500, 2006BAB18B03, and 2006BAB18B05), by CMA (GYHY(QX)2007-6-5),

by NSFC (40233032), and by the Centurial Program sponsored by the Chinese Academy of Sciences. The work described in this publication was also supported by the European Commission (Call FP7-ENV-2007-1 Grant nr. 212921) as part of the CEOP – AEGIS project (http://www.ceop-aegis.org/) coordinated by the Université Louis Pasteur. The National Center for Atmospheric Research is sponsored by the National Science Foundation.

References

Adams, J. M., Faure, H., Faure-Denard, L., McGlade, J. M., and Woodward, F. I.: Increases in terrestrial carbon storage from the Last Glacial maximum to the present, Nature 348, 711–714, 1990.

Baldocchi, D. D. and Vogel, C. A.: Seasonal variation of energy and water vapor exchange rates above and below a boreal jack pine forest canopy, J. Geophys. Res., 102(D24), 28939–28951, 1997.

Baldocchi, D. D., Vogel, C. A., and Brad, H.: Seasonal variation of carbon dioxide exchange rates above and below a boreal jack pine forest, Agr. Forest Meteorol., 83, 147–170, 1997.

Baldocchi, D. D., Falge, E., Gu, L. H., et al.: Fluxnet: a new tool to study the temporal and spatial variability of ecosystem-scale carbon dioxide, water vapor, and energy flux densities, B. Am. Meteorol. Soc., 82, 2415–2434 , 2001.

Barros, A. P., Munoz, F., Wood, A. W., Voisin, N., Bohn, T., Rodriguez, J. C., Lettenmaier, D. P., Burges, S. S., and Watts, C. J.: Monitoring the diurnal cycle of land-atmosphere interactions in Sonora, Mexico during NAME/SMEX04, AMS Conference on Hydrology, 19, 2005.

Beljaars, A. C. M. and Holtslag, A. A. M.: Flux parameterization over land surfaces for atmospheric models, J. Appl. Meteorol., 30, 327–341, 1991.

Betts, A. K. and Ball, J. H.: The FIFE surface diurnal cycle climate, J. Geophys. Res., 100(D12), 679–693, 1995.

Bi, X., Gao, Z., Deng, X., Wu, D., Liang, J., Zhang, H., Sparrow, M., Du, J., Li, F., and Tan, H.: Seasonal and diurnal variations in moisture, heat and CO_2 fluxes over grassland in the tropical monsoon region of southern China, J. Geophys. Res., 112, D10106, doi:10.1029/2006JD007889, 2007.

Burba, G. G., Verma, S. B., and Kim, J.: Surface energy fluxes of Phragmites australis in a prairie wetland, Agr. Forest Meteorol., 94, 31–51, 1999.

Campbell, C. S., Heilman, J. L., McInnes, K. J., Wilson, L. T., Medley, J. C., Wu, G. W., and Cobos, D. R.: Diel and seasonal variation in CO_2 flux of irrigated rice, Agr. Forest Meteorol., 1, 108, 15–27, 2001.

Delire, C and Gerard, J. G.: A numerical study of the influence of the diurnal cycle on the surface energy and water budgets, J. Geophys. Res., 100(D3), 5071–5084, 1995.

Desai, A. R., Noormets, A. N., Bolstad, P. V., Chen, J., Cook, B. D., Davis, K. J., Euskirchen, E. S., Gough, C. M., Martin, J. G., Ricciuto, D. M., Schmid, H. P., Tang, J. W., and Wang, W.: Influence of vegetation and surface forcing on carbon dioxide fluxes across the Upper Midwest, USA: Implications for regional scaling, Agr. Forest Meteorol., 288–308, doi:10.1016/j.agrformet.2007.08.001, 2008.

Dickinson, R. E., Hendersin-Sellers, A., Rosenzweig, C., and Sellers, P. J.: Evapotranspiration models with canopy resistance for use in climate models, a review, Agr. Forest Meteorol., 54, 373–388, 1991.

Dugas, W. A., Heuer, M. L., and Msyeux, H. S.: Carbon dioxide fluxes over Bermuda grass, native prairie, and sorghum, Agr. Forest Meteorol., 93, 121–139, 1999.

Foken, T. and Oncley, S. P.: Results of the workshop "Instrumental and methodical problems of land surface flux measurements", B. Am. Meteorol. Soc., 76, 1191–1193, 1995.

Foken, T., Kukharets, V. P., Perepelkin, V. G., Tsvang, L. R., Richter, S. H., and Weisensee, U.: The influence of the variation of the surface temperature on the closure of the surface energy balance, 13th Symposium on Boundary Layer and Turbulence, Dallas, TX., 10–15 January 1999, Amer. Meteorol. Soc., 308–309, 1999.

Frank, A. B. and Dugas, W. A.: Carbon dioxide fluxes over a northern, semiarid, mixed grass prairie. Agr. Forest Meteorol. 108, 317–326, 2001.

Gao, Z., Bian, L., and, Zhou, X.: Measurements of turbulent transfer in the near-surface layer over a rice paddy in China, J. Geophys. Res., 108(D13), 4387, dio:10.1029/2002JD002779, 2003.

Gao, Z.: Determination of soil heat flux in a Tibetan short-grass prairie, Bound.-Lay. Meteorol., 114, 165–178, 2005.

Gao, Z., Horton, R., Liu, H. P., Wen, J., and Wang, L.: Influence of wave phase difference between surface soil heat flux and soil surface temperature on land surface energy balance closure, Hydrol. Earth Syst. Sci. Discuss., 6, 1089–1110, 2009, http://www.hydrol-earth-syst-sci-discuss.net/6/1089/2009/.

Garratt, J. R.: The Atmospheric Boundary Layer, Cambridge University Press, Cambridge,

316 pp., 1992.
Hao, Y., Wang, Y., Huang, X., Cui, X., Zhou, X., Wang, S., Niu, H., and Jiang, G.: Seasonal and interannual variation in water vapor and energy exchange over a typical steppe in Inner Mongolia, China, Agr. Forest Meteorol., 146, 57–69, 2007.
Harazono, Y., Kim, J., Miyata, A., Choi, T., Yun, J.-I., and Kim, J.-W.: Measurement of energy budget components during the International Rice Experiment (IREX) in Japan, Hydrol. Process., 12, 2018–2092, 1998.
Hartog, G. D. and Neumann, H. H.: Energy budget measurements using eddy correlation and Bowen ratio techniques at the Kinosheo Lake tower site during the Northern Wetlands Study, J. Geophys. Res., 99, D1, 1539–1549, 1994.
Horst, T. W. and Weil, J. C.: How far is far enough? The fetch requirements for micrometeorological measurement of surface fluxes, J. Atmos. Ocean. Tech., 11, 1019–1025, 1994.
Intergovernmental Panel on Climate Change, Climate Change 1995: The Science of Climate Change, edited by Houghton, J. T., Meira Filho, L. G., Callander, B. A., Harris, N., Kattenberg, A., Maskell, K., Cambridge Univ. Press, New York, 1995.
Kahan, D. S., Xue, Y., and Allen, S. J.: The impact of vegetation and soul parameters in simulations of surface energy and water balance in the semi-arid sahel: A case study using SEBEX and HAPEX-Sahel data, J. Hydrol., 320, 238–259, 2006.
Kaimal, J. C. and Finnigan, J.: Atmospheric Boundary Flows, Their Structure and Measurement, Oxford Univ. Press, New York, 1994.
Li, S., Werner, E., Asanuma, J., Kotani, A., Davaa, G., Dambaravjaa, O., and Michiaki, S.: Energy partitioning and its biophysical controls above a grazing steppe in central Mongolia. Agr. Forest Meteorol., 137, 89–106, 2006.
Merquiol, E., Pnueli, L., Cohen, M., Simovitch, M., Rachmilevitch, S., Goloubinoff, P., Kaplan, A, and Mittler, R.: Seasonal and diurnal variations in gene expression in the desert legume Retama raetam, Plant Cell Environ., 25, 1627–1638, 2002.
Mielnick, P. C., Dugas, W. A., Johnson, H. B., Polley, H. W., and Sanabria, J.: Net grassland carbon flux over a subambient to superambient CO_2 gradient, Glob. Change Biol., 7, 747–754, 2001.
Moore, C. J.: Frequency response to corrections for eddy correlation system. Bound.-Lay. Meteorol., 37, 17–35, 1986.
Novick, K. A., Stoy, P. C., Katul, G. G.: Carbon dioxide and water vapor exchange in a warm temperate grassland, Oecologia, 138, 259–274, 2004.

Oncley, S. P., Foken, T., Vogt, R., Kohsiek, W., DeBruin, H. A. R., Bernhofer, C., Christen, A., van Gorsel, E., Grantz, D., Feigenwinter, C., Lehner, I., Liebethal, C., Liu, H., Mauder, M., Pitacco, A., Ribeiro, L., and Weidinger, T.: The energy balance experiment EBEX-2000. Part 1: overview and energy balance, Bound.-Lay. Meteorol., 123, 1–28, doi:10.1007/s10546-007-9161-1, 2007.

Panin, G. N., Tetzlaff, G., Raabe, A., Schönfeld, H. J., Nasonov, A. E.: Inhomogeneity of the land surface and the parametrization of surface fluxes – a discussion, Wiss. Mitt. aus dem Inst. für Meteorol. der Univ. Leipzig und dem Institut für Troposphärenforschung e.V. Leipzig, 4, 204–215, 1996.

Rowntree, P. R.: Atmospheric parameterization schemes for evaporation over land: basic concepts and climate modeling aspects, in Land Surface Evaporation, Measurement and Parameterization, edited by: Schmugge, T. J. and Andre, J. C., 5–29., Springer-Verlag, New York, 1991.

Schmid, H. P.: Source areas for scalars and scalar fluxes, Bound.-Lay. Meteorol., 67, 293–318, 1994.

Schuepp, P. H., Leclerc, M. Y., MacPherson, J. I., and Desjardins, R. L.: Footprint prediction of scalar fluxes from analytical solution of the diffusion equation, Bound.-Lay. Meteorol., 50, 355–373, 1990.

Sims, P. L. and Bradford, J. A.: Carbon dioxide fluxes in a southern plains prairie, Agr. Forest Meteorol., 109, 117–134, 2001.

Steven, J. H., Walter, C. O., and Arturo, M. M.: Diurnal, seasonal and annual variation in the net ecosystem CO_2 exchange of a desert shrub community (Sarcocaulescent) in Baja California, Mexico, Glob. Change Biol., 11, 927–939, 2005.

Su, Z., Timmermans, W., Gieske, A., Jia, L., Elbers, J. A., Olioso, A., Timmermans, J., Van Der Velde, R., Jin, X., Van Der Kwast, H., Nerry, F., Sabol, D., Sobrino, J. A., Moreno, J., and Bianchi, R.: Quantification of land-atmosphere exchanges of water, energy and carbon dioxide in space and time over the heterogeneous Barrax site, Int. J. Remote Sens., 29, 17, 5215–5235, 2008.

Suyker, A. E. and Verma, S. B.: Year-round observations of the net ecosystem exchange of carbon dioxide in a native tallgrass prairie, Glob. Change Biol., 7, 279–289, 2001.

Toda, M., Nishida, K., Ohte, N., Tani, M., and Musiake, K.: Observations of Energy Fluxes and Evapotranspiration over Terrestrial Complex Land Covers in the Tropical Monsoon Environment, J. Meteorol. Soc. Jpn., 80, 3, 465–484, 2002.

Vourlitis, G. L., Filho, N. P., Hayashi, M. M. S., Nogueira, J. De. S., Caseiro, F. T., and Campelo, J. H.: Seasonal variations in the net ecosystem CO_2 exchange of a mature Amazonian transitional tropical forest (cerradão), Funct. Ecol., 15, 388–395, 2001.

Webb, E. K., Perman, G. I., and Leuning, R.: Correction of flux measurements for density effects due to heat and water transfer, Q. J. Roy. Meteor. Soc., 106, 85–100, 1980.

Wever, L. A., Flanagan, L. B., and Carlson, P. J.: Seasonal and interannual variation in evapotranspiration, energy balance, and surface conductance in northern temperate grassland, Agr. Forest Meteorol., 112, 31–49, 2002.

Wicke, W. and Bernhofer, C.: Energy balance comparison of the Hartheim Forest and an adjacent grassland site during the HartX Experiment, Theor. Appl. Climatol., 53, 49–58, 1996.

Woodward, F. L., Lomas, M. R., and Betts R. A.: Vegetation-climate feedbacks in a greenhouse world, Philos. T. Roy. Soc., 353, 29–39, 1998.

Xue, Y., Juang, H. M., Li, W., Prince, S., DeFries, R., Jiao, Y., and Vasic, R.: Role of land surface processes in monsoon development: East Asia and West Africa, J. Geophys. Res., 109, D03105, doi:10.1029/2003JD003556, 2004.

Fig. 1. Photo of the setup at the measurement site.

HESSD

6, 1939–1972, 2009

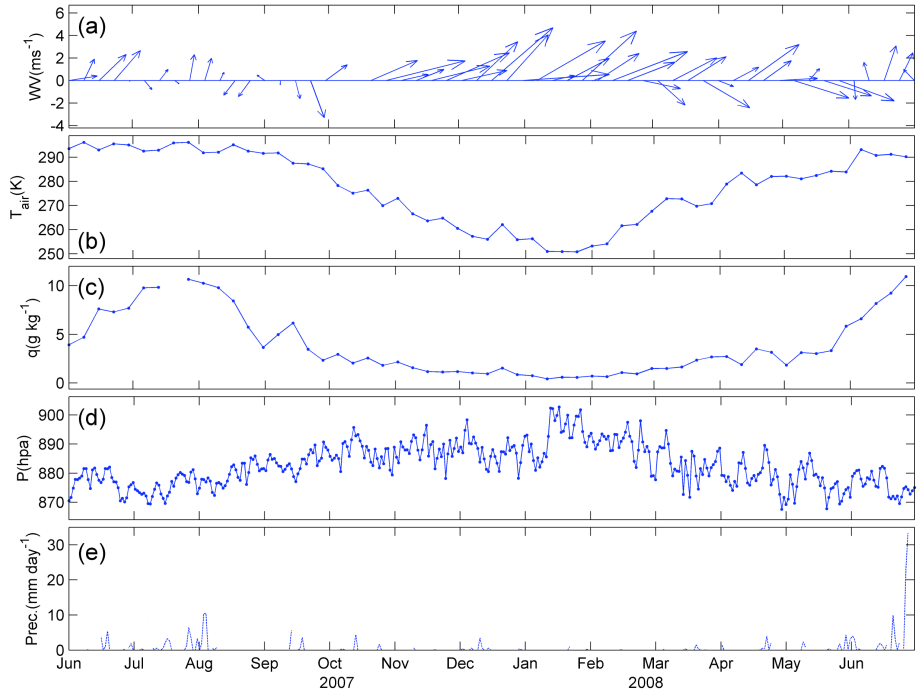

Fig. 2. Meteorological data collected at the grassland site during the period from June 2007 to June 2008 at the steppe prairie site.

HESSD

6, 1939–1972, 2009

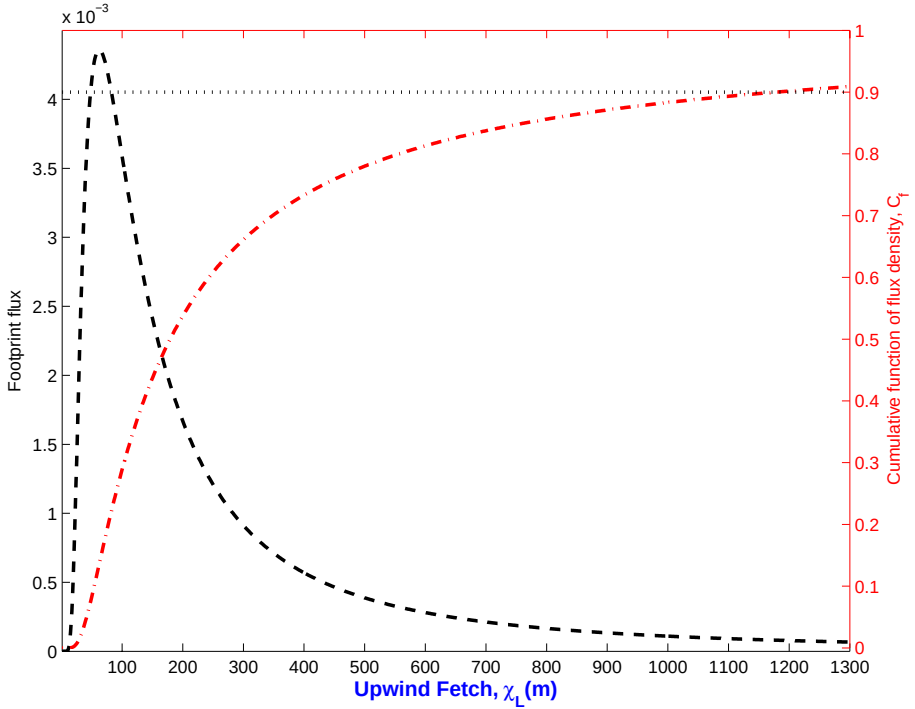

Fig. 3. Footprint flux and contributions of the cumulative flux according to Eq. (5) for neutral stability where U=3.98 m s^{-1}, z=4.0 m, d=0.2 m, and u_*=0.30 m s^{-1}.

HESSD
6, 1939–1972, 2009

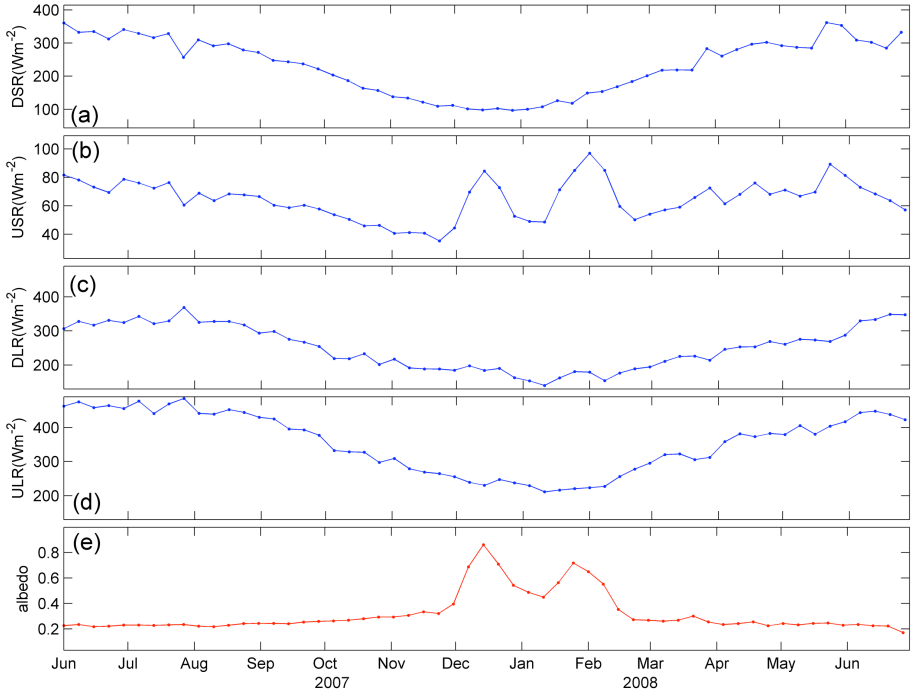

Fig. 4. Seasonal variations of weekly mean downward shortwave radiation (DSR), upward shortwave radiation (USR), downward longwave radiation (DLR), upward longwave radiation (ULR) and surface albedo during the period from June 2007 to June 2008 at the steppe prairie site.

HESSD

6, 1939–1972, 2009

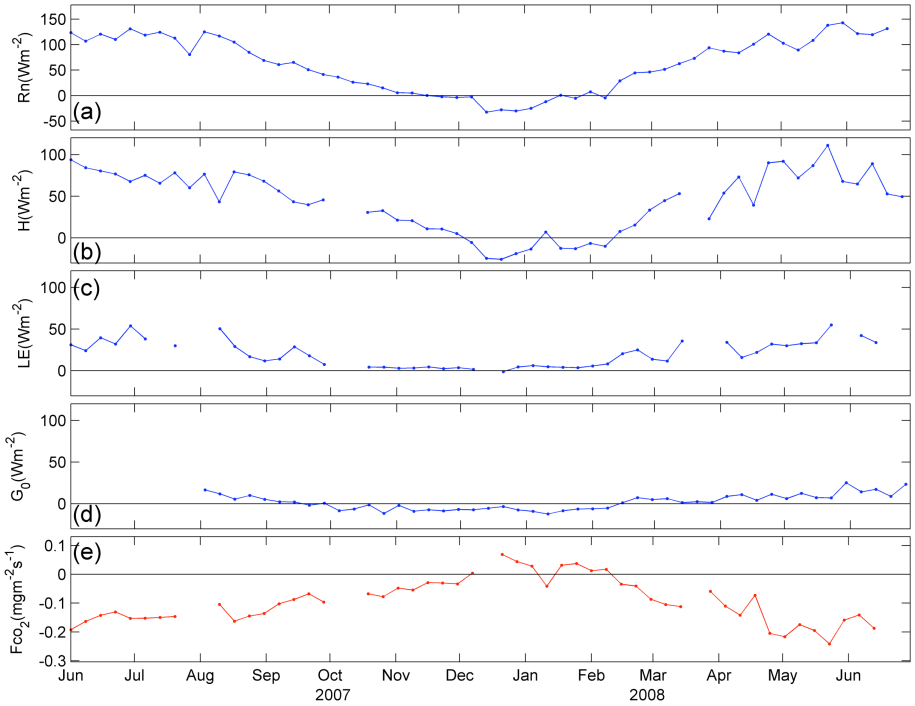

Fig. 5. Seasonal variations of weekly mean net radiation (*Rn*), sensible heat flux (*H*), latent heat flux (*LE*), soil heat flux (G_0) and CO_2 flux (F_{CO_2}) during the period from June 2007 to June 2008 at the steppe prairie site.

HESSD

6, 1939–1972, 2009

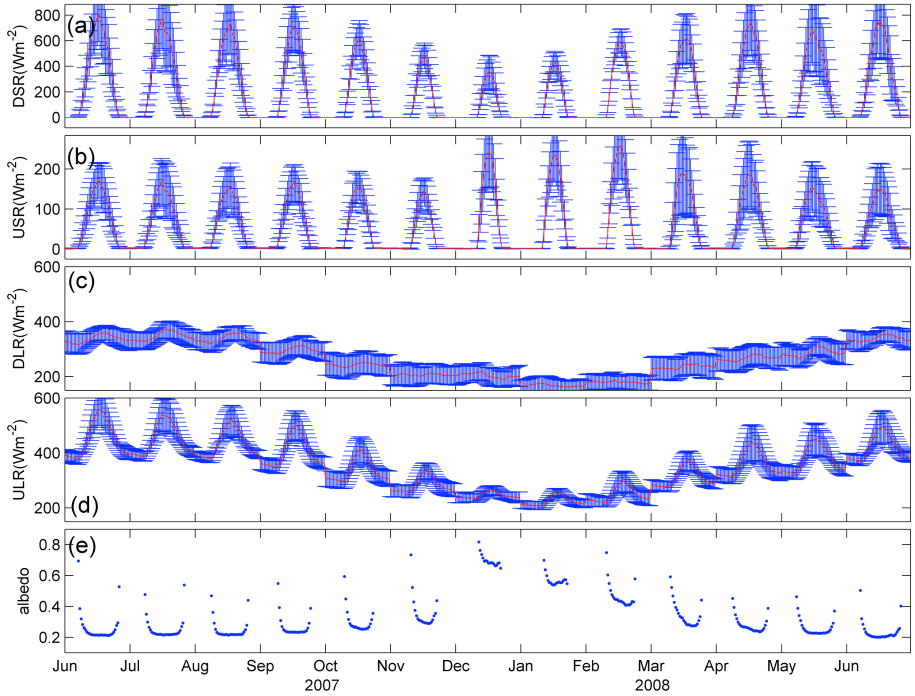

Fig. 6. Diurnal variations of weekly mean downward shortwave radiation (DSR), upward shortwave radiation (USR), downward longwave radiation (DLR), upward longwave radiation (ULR) and surface albedo during the period from June 2007 to June 2008 at the steppe prairie site.

HESSD

6, 1939–1972, 2009

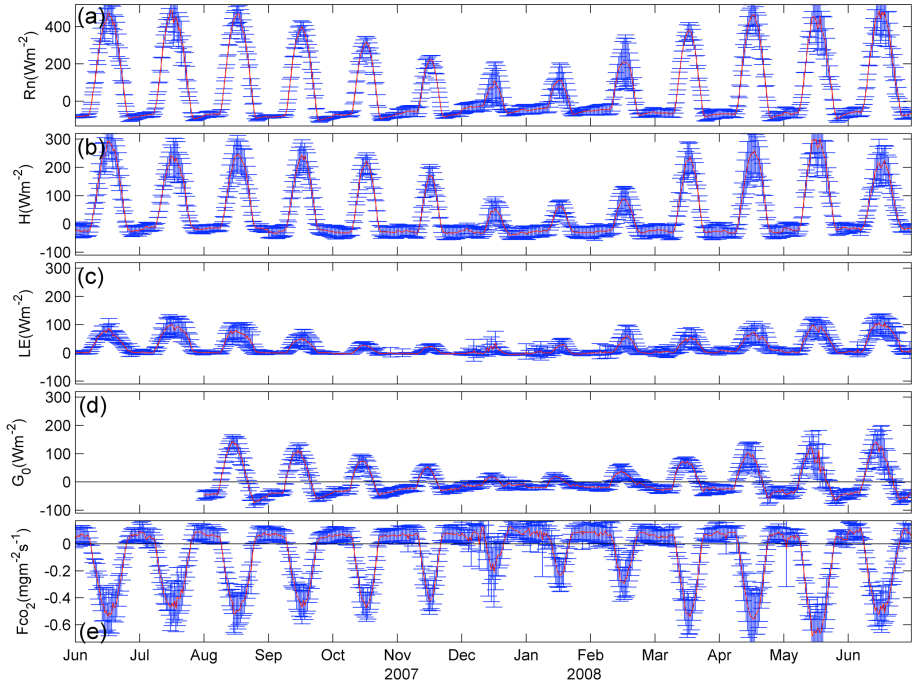

Fig. 7. Diurnal variation of weekly mean net radiation (*Rn*), sensible heat flux (*H*), latent heat flux (*LE*), soil heat flux (G_0) and CO_2 flux (F_{CO_2}) during the period from June 2007 to June 2008 at the steppe prairie site.

HESSD

6, 1939–1972, 2009

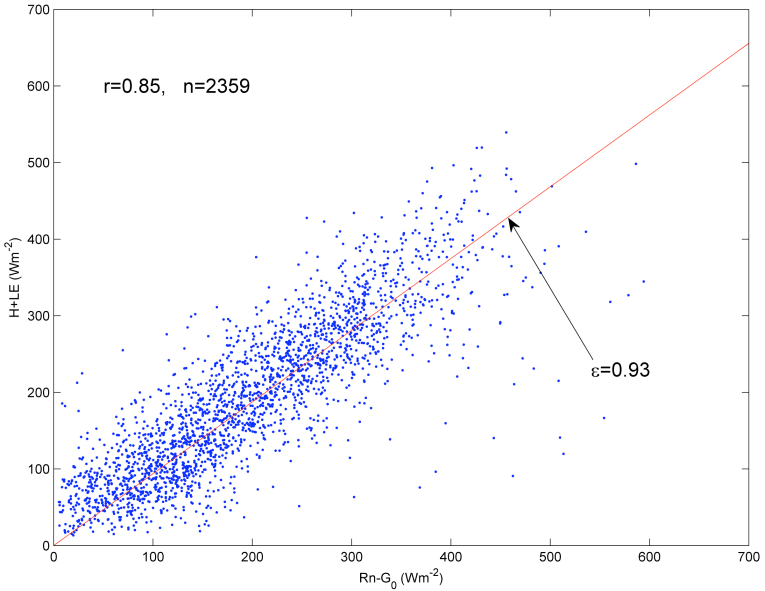

Fig. 8. Inter-comparison of the measured ($H+LE$) against available energy ($Rn-G_0$) during the period from June 2007 to June 2008 at the steppe prairie site.

HESSD

6, 1939–1972, 2009

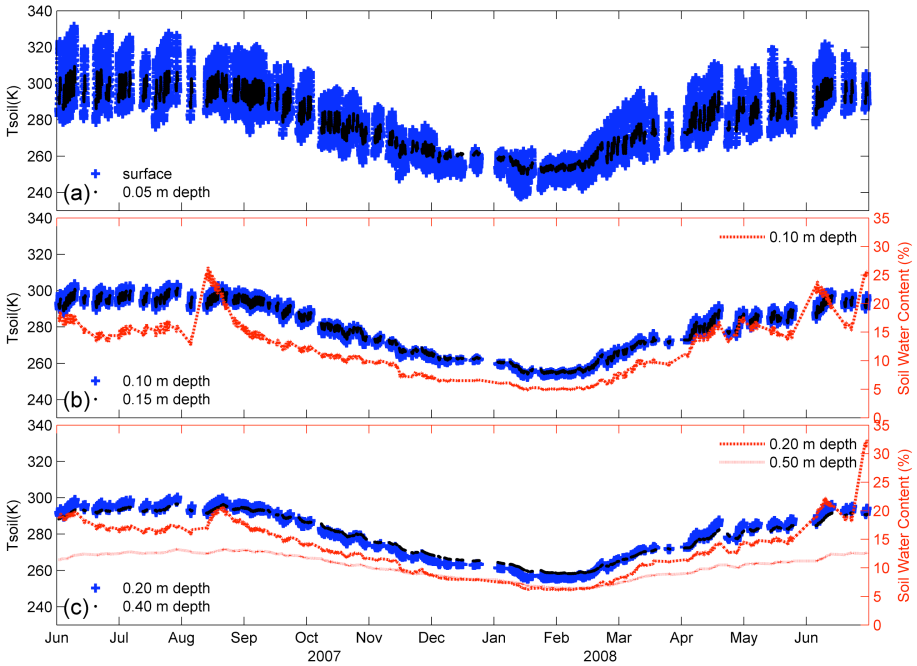

Fig. 9. Temporal variations of soil surface temperature (K) and at the depths of 0.05, 0.10, 0.15, 0.2, and 0.4 m, and of soil water content at the depths of 0.10, 0.20, and 0.5 m.

HESSD

6, 1939–1972, 2009

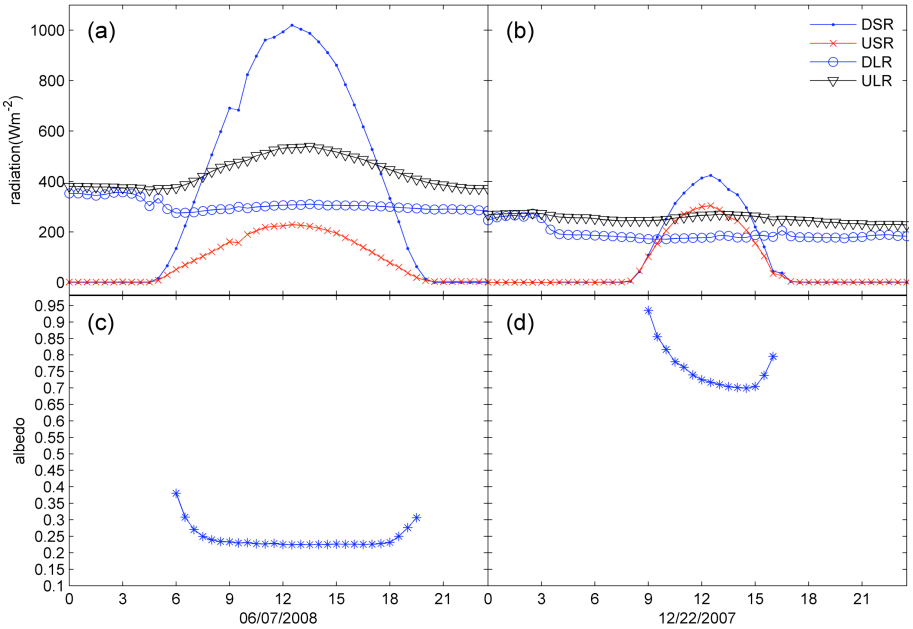

Fig. 10. Diurnal variation of downward shortwave radiation (DSR), upward shortwave radiation (USR), downward longwave radiation (DLR), upward longwave radiation (ULR) and surface albedo on 7 June 2008, and on 22 December 2007 at the steppe prairie site.

HESSD
6, 1939–1972, 2009

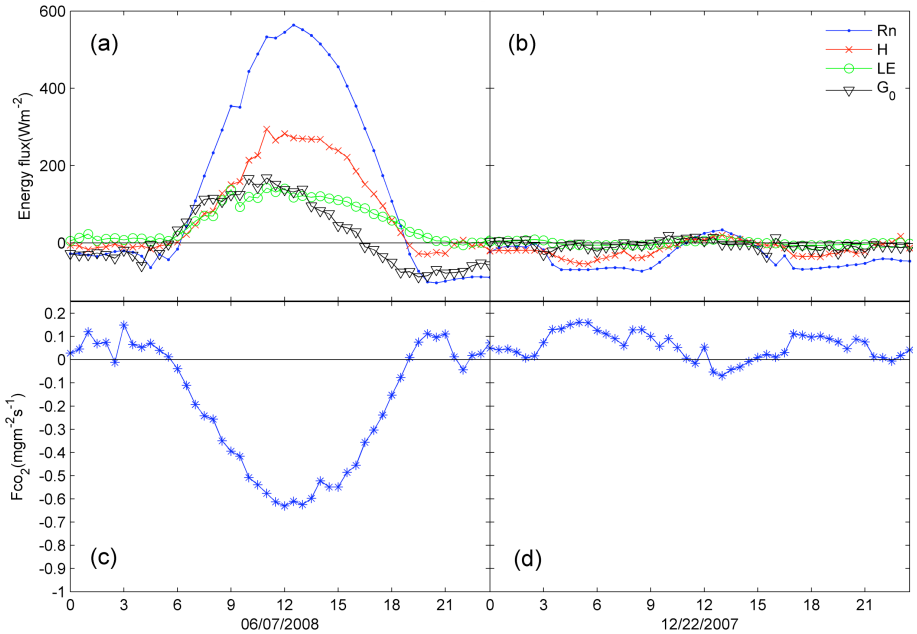

Fig. 11. Diurnal variations of net radiation (*Rn*), sensible heat flux (*H*), latent heat flux (*LE*), soil heat flux (G_0), and CO_2 flux (F_{CO_2}) on 7 June 2008 and on 22 December 2007 at the steppe prairie site.

HESSD
6, 1939–1972, 2009

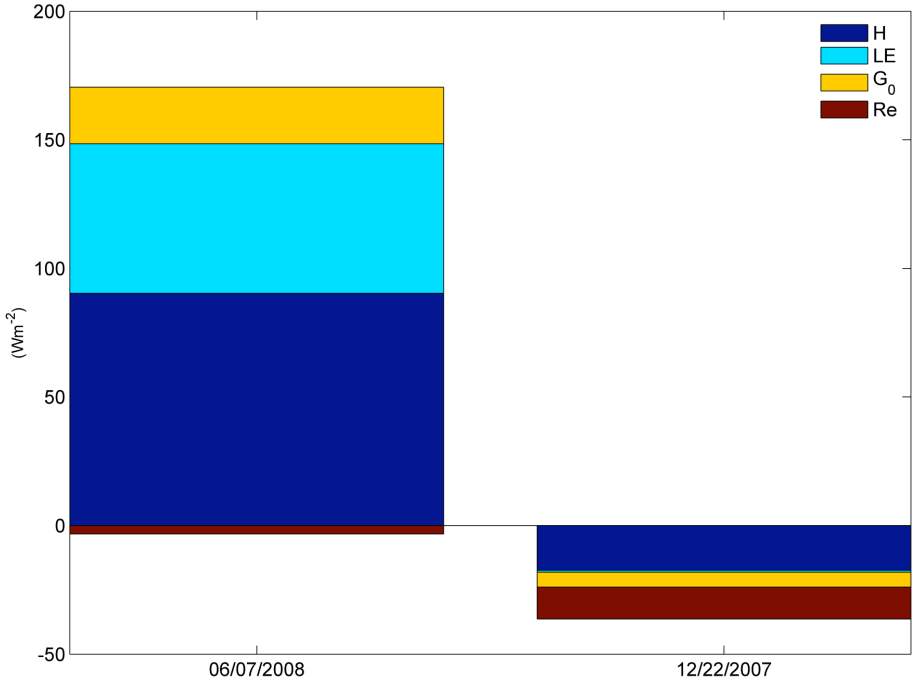

Fig. 12. Surface energy partitioning on 7 June 2008 and on 22 December 2007 at the steppe prairie site.

HESSD

6, 1939–1972, 2009